G. Kapper et al.

Modelling of Electron Cyclotron Current Drive for Finite Collisionality Plasmas in Wendelstein 7-X

Modeling of electron cyclotron current drive
for finite collisionality plasmas in Wendelstein 7-X

G. Kapper[1], W. Kernbichler[1], S.V. Kasilov[1,2], N.B. Marushchenko[3]

[1] *Fusion@ÖAW, Institute of Theoretical and Computational Physics, TU Graz, Austria*

[2] *Institute of Plasma Physics, National Science Center "Kharkov Institute of Physics and Technology", Ukraine*

[3] *Max Planck Institute for Plasma Physics, EURATOM Association, Germany*

Introduction

The low-shear concept of Wendelstein 7-X avoids low-order rational flux surfaces in the plasma core since large magnetic islands can be formed there. In turn, such a resonant surface is placed at the plasma edge, thus producing an island divertor configuration. In order to preserve these features, which can be destroyed even by the arise of a relatively small bootstrap current, this current should be compensated by electron cyclotron current drive (ECCD) [1]. In modern fusion devices the evaluation of the generalized Spitzer function (GSF), which serves as an ECCD efficiency, is usually performed in the low collisionality limit typical for these devices, where one can effectively use the bounce averaged kinetic equation. At the same time, at high densities and mild electron temperatures, which can be expected at the initial stage of the device operation and at the start up of plasma discharge, finite collisionality effects should be taken into account. Such an approach requires the solution of the high dimensional (4D) drift kinetic equation, which is a more difficult task as compared to the 2D bounce averaged equation. In this work, the impact of finite collisionality effects on ECCD in a high-mirror configuration of Wendelstein 7-X is studied using a combination of the codes NEO-2 [2], a 4D drift kinetic equation solver for plasmas with finite collisionality using the full linearized Coulomb collision operator and realistic device geometry, and TRAVIS [3], a ray-tracing code developed for studies of electron cyclotron current drive, heating and emission. Recently, this code combination was used to study the influence of finite collisionality on ECCD in tokamaks, where the generalized Spitzer problem at a given magnetic flux surface is essentially 3D [2]. The 4D problem of stellarators led to the development of a new interface between the codes based on precomputed data of NEO-2 for a realistic magnetic model from an equilibrium code and plasma parameter profiles from a transport code. As in Ref. [2], the non-relativistic limit is used here for the GSF, which is compared to asymptotic limits of low and high plasma collisionality.

Code combination within the adjoint approach

A commonly used technique for current drive modeling is the adjoint approach [4], where the flux surface averaged parallel current density,

$$\langle j_\parallel B \rangle = e\, l_c \left\langle \int \mathrm{d}^3 p\, \frac{\partial \bar{g}}{\partial \mathbf{p}} \cdot \mathbf{\Gamma}_{\mathrm{RF}} \right\rangle, \tag{1}$$

is expressed by an adjoint GSF $\bar{g}$ computed by NEO-2 and a microwave induced quasilinear diffusion flux in phase space $\mathbf{\Gamma}_{\mathrm{RF}}$ computed by TRAVIS, where $\langle \ldots \rangle$ denotes flux surface average, e is the electron charge, B is the magnetic field module and l_c is the mean free path [2]. The adjoint function is related by $\bar{g}(v_\parallel) = -g(-v_\parallel)$ to the usual GSF g, which is a solution to the conductivity problem written in terms of integrals of motion in velocity space as follows,

$$v_\parallel \mathbf{h} \cdot \nabla f_{\mathrm{M}} g - \hat{L}_{\mathrm{CL}} f_{\mathrm{M}} g = \frac{B}{l_c} v_\parallel f_{\mathrm{M}}. \tag{2}$$

Here, $v_\parallel$ is the parallel velocity, $\mathbf{h}$ is a unit vector along the magnetic field, f_{M} is a Maxwellian and $\hat{L}_{\mathrm{CL}}$ is a linearized collision integral. Cross-field rotation has been ignored in Eq. (2) because it has small effect on the GSF in finite collisionality regimes as well as at low collisionalities where the electrons are mostly in the $1/v$ regime. Therefore, a 4D problem (2) can be reduced to a 3D problem for a single field line (position on field line is given by a line parameter φ_s) which is long enough to cover the given flux surface (labeled by the normalized toroidal flux value s) densely. Representing the energy dependence of the GSF $g(\mathbf{r}, \mathbf{p})$ by a series expansion over normalized Laguerre polynomials of the order $3/2$ (Sonine polynomials) $L_m^{(3/2)}(z)$, the solution to Eq. (2) is

$$g(\mathbf{r}, \mathbf{p}) = \sum_{m=0}^{M} g_m(\varphi_s, \eta) L_m^{(3/2)}(z), \tag{3}$$

where $\eta = p_\perp^2/(p^2 B)$ and $z = p^2/(2mT) = mv^2/(2T)$ are the normalized perpendicular adiabatic invariant and energy, respectively. The GSF expansion coefficients $g_m(\varphi_s, \eta)$ are computed by NEO-2 using a conservative finite difference scheme on a 2D grid over φ_s and η with an adaptively refined η-grid in order to resolve the trapped-passing boundary layer. The spatial dependence of g on Boozer coordinates (s, ϑ, φ) required by TRAVIS is reconstructed by an interface with the help of linear interpolation on a non-uniform 3D grid formed by (discretized over φ_s) segments of (long enough) field lines representing a prescribed set of flux surfaces.

Results

In this work, two ECCD scenarii in W7-X, namely the X2- and the O2-scenario, are investigated for three different collision models, i.e., long mean free path (LMFP) limit by the internal
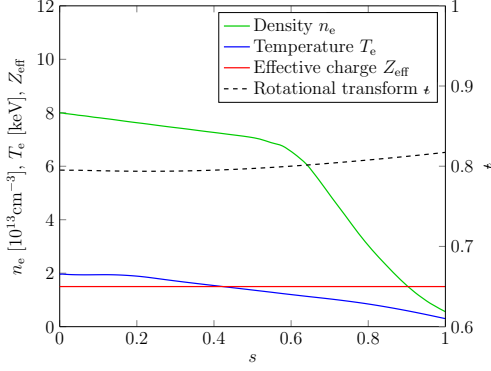
Figure 1: *Temperature, density, effective charge and rotational transform profiles over the normalized toroidal flux.*

TRAVIS model, finite collisionality by NEO-2 and the high-collisional limit using the classical Spitzer function [5]. Profiles of plasma parameters shown in Fig. 1 correspond to the onset of the LMFP regime (collisionality is roughly three times smaller than needed for the plateau regime). The microwave beam is launched off axis ($Z = -0.1$ m) in the horizontal plane with the poloidal launch angle $\alpha = 5.5$ deg (angle between this plane and the beam). Dependencies of the total current generated in the plasma on the toroidal launch angle β (angle between the beam and the meridian plane containing the launcher) are shown in Fig. 2. It can be seen that in the standard X2-scenario the current is by 25% different from the LMFP limit, as it can be expected, while for the advanced O2-scenario the current significantly differs from both, LMFP and high collisionality limits. In the latter case, characterized by weak absorption and respectively smaller current, a significant part of this current is produced by particles from the trapped region. This is better seen from Fig. 3 where the distributions of the absorbed power and generated current along the microwave beam are shown for $\beta = 18.5$ deg. Due to the strong absorption in the X2 case, most power is absorbed by strongly passing particles, whose distribution function is not significantly different from the GSF in the LMFP limit, before the beam reaches the cold resonance. In the O2-scenario weak absorption results in power absorption and respective counter-current by passing particles on the other side of cold resonance, as well as in a significant amount of wave energy absorbed by trapped particles whose current is mainly determined by the position of the absorption region but not significantly by the parallel wave number [6, 2]. This can be used to increase the total toroidal current.
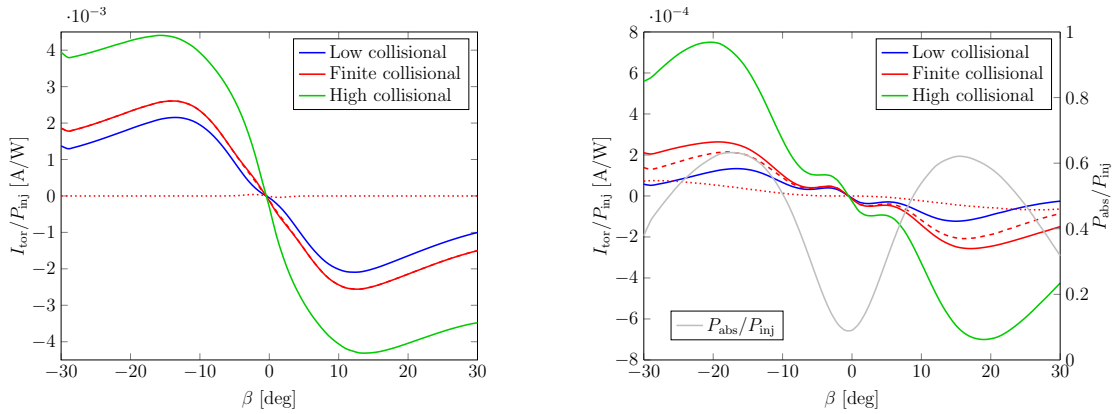

Figure 2: *Total toroidal current by passing (dashed), trapped (dotted) and all (solid) particles as function of the toroidal launch angle β for X2-mode (left) and O2-mode (right). The fraction of the absorbed power P_{abs}/P_{inj} is shown for the O2-mode only, since for the X2-mode there is total absorption.*
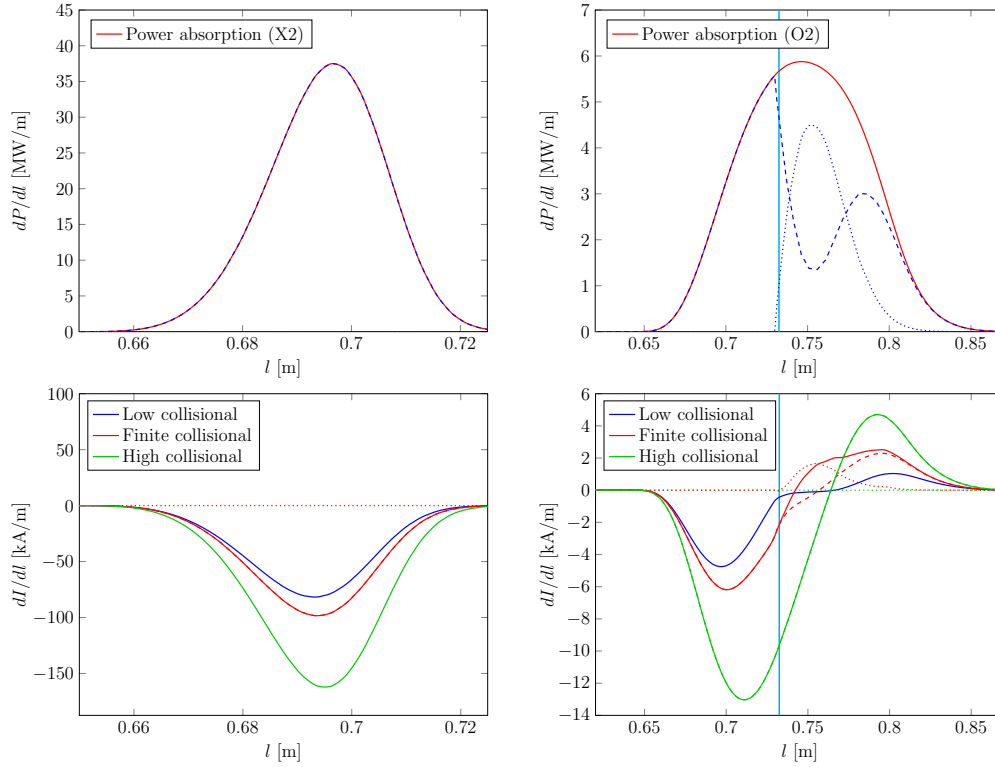
Figure 3: *Local power absorption (upper plots) and local current generation (lower plots) for X2-mode (left) and O2-mode (right) by passing (dashed), trapped (dotted) and all (solid) particles along the ray trajectory. Cold resonance position at l = 0.73 m is marked by a vertical (cyan) line.*

Conclusion

This report extends the ECCD studies for tokamaks [2] to stellarator geometry. The studies of the X2- and O2-scenarii in a high-mirror configuration of W7-X at the onset of the LMFP regime show that in the O2-scenario finite collisionality effects play a significant role on ECCD current, which cannot be approximated by asymptotical collisionality limits. This effect is significant also in the X2-scenario, where the current is increased by 25%. Properties of ECCD on trapped particles can be used to improve the efficiency in advanced (O2, X3) scenarii, which are only available at high densities, where the cut-off prohibits the standard (O1, X2) scenarii.

Acknowledgments

References

[1] M. Romé, *et al.*, *Plasma Phys. Control. Fusion* **40**(4), 511 (1998)

[2] W. Kernbichler, *et al.*, *EPJ Web of Conferences* **87**, 01006 (2015)

[3] N. B. Marushchenko, *et al.*, *Comput. Phys. Commun.* **185**(1), 165 (2014)

[4] T. M. Antonsen and K. R. Chu, *Phys. Fluids* **25**(8), 1295 (1982)

[5] L. Spitzer, Jr. and R. Härm, *Phys. Rev.* **89**(5), 977 (1953)

[6] P. Helander and P. J. Catto, *Phys. Plasmas* **8**(5), 1988 (2001)